Transactions of the Materials Research Society of Japan 29[5] 2499-2502 (2004)

Relationship between the Piezoelectric Phenomenon and the Mechanical Behavior under Combined Compression and Vibration Stresses

Takahisa NAKAI*, Masatoshi HAMATAKE**, and Tetsuya NAKAO***

* Department of Natural Resources Process Engineering, Shimane University,
1060 Nishikawatsumachi, Matsue, Shimane 690-8504, Japan
Fax: 81-852-32-6071, e-mail: jaja@riko.shimane-u.ac.jp

** Tsuda Forest Industrial Corporation
1-8-19 Hirabayashi-minami, Suminoe, Osaka, Osaka 559-0025, Japan
Fax: 81-6-6684-2607, e-mail: hamage007@hotmail.com

*** Department of Natural Resources Process Engineering, Shimane University,
1060 Nishikawatsumachi, Matsue, Shimane 690-8504, Japan
Fax: 81-852-32-6123, e-mail: nakaote@riko.shimane-u.ac.jp

Abstract: In this study, the piezoelectric phenomenon in wood subjected to deformation processes and the relationship between the piezoelectric voltage (*P*) and microscopic fractures in the wood were investigated. In particular, the deformation of the cross-sectional wall of the tracheid under combined compression and vibration stresses was examined. The piezoelectric voltage-displacement (*P-D*) curve consisted of a linear region that started from the origin, followed by a convex curved region. In the elastic region, the *P-D* curve and the first derivatives of the load-displacement (*L-D*) curves were fairly similar. When stresses were applied to a specimen, the cross-sectional walls of the tracheid were deformed mainly at the radial walls. The elastic buckling stress of the cross-sectional wall of the tracheid was estimated from scanning electron microscope images and by assuming that the tracheid was approximately a hexagonal prism. The results indicated that the *P-D* curve transitioned from the linear region to the convex curved region as soon as the radial wall of the tracheid buckled elastically. The maximum point of the *P-D* curve in the elastic region almost corresponded with the proportional limit of the *L-D* curve. After reaching the proportional limit of the *L-D* curve, the value of *P* decreased gradually. The specimens showed a clear peak in the *P* curve that originated from the inhomogeneous strain.

Key words: Combined compression and vibration stresses, Piezoelectric voltage, Elastic buckling stress, Inhomogeneous strain

1. INTRODUCTION

It is generally accepted that the piezoelectric effect in wood is caused by the natural cellulose crystals in the cell wall. However, natural cellulose cannot exist as a molecule in wood. Many molecular chains of cellulose form fiber structures in bundles with hemicellulose and lignin, *i.e.*, microfibrils. The cell wall can be considered as a frame for these microfibrils. Hence, the increase and decrease of the piezoelectric voltage during the deformation of wood originates from the dynamic deformation of the cell wall.

Many studies of the piezoelectric effect in wood have examined the physical properties of small specimens of wood under a minute load, but there has been very little research on deformation [1-4]. Therefore we examined test specimens subjected to combined compression and vibration stresses at a 45-degree angle to the fiber and load directions to clarify the relationship between the piezoelectric voltage and deformation in the elastic and plastic regions. In particular, the piezoelectric voltage-displacement (*P-D*) curve was generated, and the correspondence between it and the load-deformation (*L-D*) curve or the aspect ratio of the deformation of the cross-sectional wall of the tracheid was investigated in detail.

2. EXPERIMENTS

The specimens used were made of kiln-dried Hinoki (*Chamaecyparis obtusa* Endl.). The size of each specimen was 0.5 × 1 × 6 cm. Four splice pieces were attached to the specimen with adhesive to hold the specimen to the jig in the chamber of the scanning electron microscope (SEM). The angle (θ) between the axial direction and the fiber direction in the specimen

was 45° . An electrode was placed on the L-R plane, and a vacuum evaporator was used to spatter platinum on the centers of the upper and lower surfaces of the specimen to act as the electrode for detecting the piezoelectric voltage. The area of the electrode was 0.75 cm^2. Silver foil, with a thickness, length, and width of 100 μm, 3 cm, and 1 mm, respectively, was used as the lead wire. The observation plane of the specimen in the SEM is shown in Figure 1. Specimens were conditioned in a desiccator with P_2O_5 after they had been vacuum dried for 24 hours.

The moisture content of the specimens was 5.7% immediately before the specimen was fixed to the jig in the chamber of the SEM and 3.5% immediately after the observations ended. The average value of the specific gravity of the specimens, ρ, before the observations was 0.43.

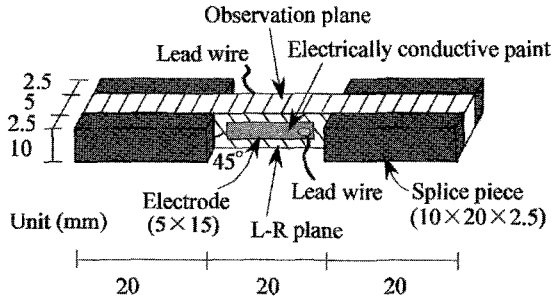

Fig. 1. Test specimen mounting.

The piezoelectric voltage generated by the wood was transmitted by the electrodes and amplified by a 1/3-octave band pass filter with an input impedance of 10 MΩ (NEC Sanei Co., Ltd.) to remove noise. The voltage was then measured with a highly sensitive alternating current voltmeter with a built-in AC-DC converter (NF Circuit Design Block Co., Ltd.). In this study, the piezoelectric voltage obtained by the measuring apparatus was an extreme value of signal. The piezoelectric voltage (load, displacement) was collected by a data acquisition controller (NEC Sanei Co., Ltd.) with a measurement speed of 100 ms integral time and stored on a personal computer.

A testing machine controlled by oil pressure (Servo pulser, full scale range = ±5 kN, Shimadzu Co., Ltd.) was used for the loading. The specimens were attached to the jig, and a static compression with a superimposed minute sinusoidal load (F), given by Equation (1) below, was applied. The order of loading was as follows: an initial load F_0 = 19.6 N was applied, then a sinusoidal load with a frequency of f = 30 Hz and an amplitude of a = 19.6 N was applied, and finally a static compression load a_0 = 0.98N was applied until the specimen failed. The sinusoidal load made it possible to detect the piezoelectric voltage with this measuring apparatus. The combined load, F, is given by:

$$F=F_0+a\sin(\omega t)+a_0 t, \quad \cdots\cdots\cdots \quad (1)$$

where t is the time from the start of the loading and ω is the angular velocity, $2\pi f$. The load cell and the stroke detector built-in to the SEM servopulser measured the compression load and the displacement. The zero point of the compression displacement was set to the position of the measuring point after the application of the initial load.

To film the condition of the specimen during the compression deformation process, the picture output from the Robinson detector (bandwidth: greater than 5 MHz; spatial resolution: better than 10 nm; useful range of accelerating voltage: 5 kV and greater; retractable distance: 63 mm) in the SEM was recorded in real-time by a video recorder (Aiwa Co., Ltd.). The image was printed using a video printer (SCT-CP220, Mitsubishi Electric Co., Ltd.).

3. RESULTS AND DISCUSSION

An example of a typical *P-D* curve obtained from this experiment is shown in Figure 2. The *P-D* curve can be classified broadly into three regions, labeled Zones A, B, and C. Zone A consists of the linear-elastic region that starts at the origin and includes the increasing part of the convex curve region. Zone B consists of the decreasing part of the convex curve region. Zone C contains some peaks in the curve. These zones are discussed in detail below using SEM images of the specimens.

3.1 Elastic Region of *P-D* curve

Typical piezoelectric voltage-displacement (*P-D*) and load-displacement (*L-D*) curves obtained from the combined compression and vibration tests are plotted in Figure 2. The figure clearly shows that the piezoelectric voltage was initially proportional to the deformation; then, the *P-D* curve became convex and increased to a maximum value. A regression analysis was performed on the linear part of the *P-D* curve, which was assumed to be an approximate straight line. The proportional limit was defined as the point where the regression line,

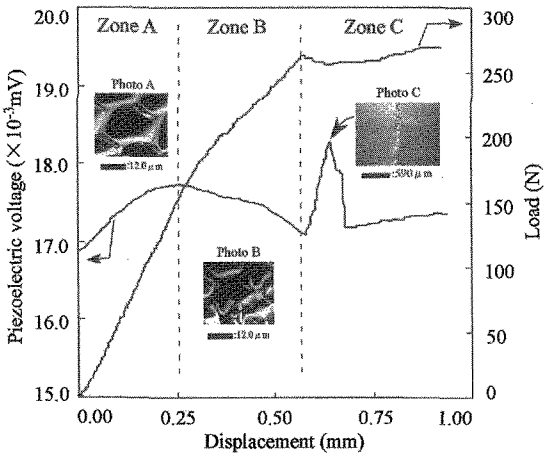

Fig. 2. Examples of the piezoelectric voltage and load – displacement curves, and the corresponding SEM images of a tracheid cross-section that has been deformed after applying the combined compression and vibration stresses.

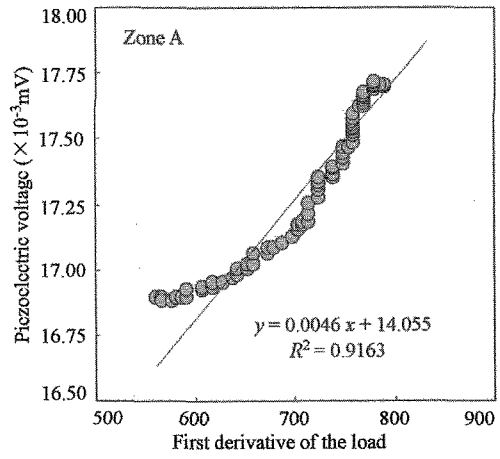

Fig. 3. Relationship between the piezoelectric voltage and the first derivative of the load.
Legend: Zone A: See Figure 2, Solid line: Regression line.

obtained from regression analysis diverged from the *P-D* curve. The load at the proportional limit of this curve was defined as $L_{P\text{-}D}$. The same analysis can be performed on the *L-D* curve to obtain $L_{L\text{-}D}$. A linear relation held between these parameters, which can be given approximately by the following equation:

$$L_{P-D}=0.58\cdot L_{L-D}. \quad \cdots\cdots\cdots \quad (2)$$

Equation (2) indicates that the linear region of the *P-D* curve was only about 60 percent of that of the *L-D* curve. After that region, the change in *P* was non-linear until the $L_{L\text{-}D}$ point. This result suggests one of the most remarkable features of the *P-D* curve. In this example, most of the *P-D* curve was non-linear since the load of the proportional limit of the *P-D* curve was only 40% of the maximum load until Zone B. Therefore, the natural cellulose crystals exhibited a non-linear elastic mechanical response. The *L-D* curve shows that the load increased with the deformation. The first derivative of the load (dL/dD (=L')) was also calculated, which corresponds to Young's modulus of the test specimen. The value of L' was not constant against the deformation, and the L'-*D* curve was convex. The *P-D* and L'-*D* curves were fairly similar. In this case, the correlation coefficient of the regression for both relationships was about 0.92, as shown in Figure 3. These results suggest the following hypothesis. In unloaded wood, the orientation of single cellulose crystals in the cellulose microfibrils is disturbed to some extent. On applying a load, the orientation of the cellulose crystalline region improves. As a result, the piezoelectric voltage and Young's modulus of the test specimens increased.

An example of a typical SEM image in Zone A is shown in Photo A of Figure 2. The photo clarifies that the combined stress load on the tracheid cross-sectional wall generates elastic buckling. In this case, no remarkable crack or fracture was observed. In a previous study [3], the tracheid was regarded as an approximate hexagonal prism so that the deformation state of the tracheid wall could be investigated using SEM images. The elastic buckling stress of the cross-sectional wall of the tracheid, σ_{cal} was calculated using the following equation:

$$\sigma_{cal.}=\frac{n^2\pi^2t^3\cos\theta_1}{12l_1^2\left(h\cos\theta_3+2l_1\sin\theta_1\right)}\cdot\frac{E}{1.50^{0.997}}, \quad \cdots \quad (3)$$

where n is a constraint condition between the cell and a neighboring cell, t is the thickness of the radial wall, l_1 and h are the lengths of the radial and tangential walls, θ_1 is the angle between the radial cell wall and the σ direction, θ_3 is the angle between the tangential cell wall and the T direction, and E is Young's modulus of the specimen. The σ_{cal} calculated from Equation (3) was plotted with the stress at the proportional limit of the *P-D* curve, $\sigma_{P\text{-}D}$. A linear relation held between these values, which could be approximated by

$$\sigma_{cal.}=0.83\cdot\sigma_{P-D}. \quad \cdots\cdots\cdots \quad (4)$$

Equations (2) and (4) indicate that the radial wall of

the tracheid generates an elastic buckling at a point equal to half the value of the load at the proportional limit. The elastic buckling stress of the radial wall of a tracheid was estimated to be only about 80% of the value of $\sigma_{P\text{-}D}$.

The measurements reported in this section were repeated to investigate whether an elastic phenomenon played a role in this result. The repeated measurements yielded a *P-D* curve with almost the same shape as the curve shown in Figure 1 during both loading and unloading. Therefore, this behavior in the elastic region resulted from both elastic and electric phenomena.

The analysis in this study was simplified by neglecting the effect of the ray parenchyma cell. However, this effect may also contribute to the buckling deformation of the tracheid radial wall. Therefore, in the future, these effects must also be examined by digitizing the deformation behavior shown in the microscopic observation results.

3.2 Non-elastic Region of *P-D* curve

In Zone B, a crack began to form at the corner of the cell wall. During this time, *P* tended to decrease slowly as the deformation progressed, and the *L-D* curve became more curved. Photo B of Figure 2 shows that the deformation of the radial walls also progressed. The walls were finally crushed as the *L-D* curve entered its plateau region in Zone C. The clear peak shown in Figure 2 appeared when this destruction had progressed across the entire width of the test specimen along the boundary of the annual ring, as shown in Photo C. This peak can be explained using the propagation theory of acoustic waves in inhomogeneous fields, as shown below [5, 6].

The combination of electrical and mechanical forces generates high order terms when the products of each power of the electrical and mechanical quantities are expressed in the coupling term. Hence, nonlinear effects must be taken into consideration, and it is necessary to consider both the linear and the higher order effects on the strain. The infinitesimal strain, u_{jk}, is described by the following equation:

$$u_{jk}=\frac{1}{2}\left(\frac{\partial u_k}{\partial a_j}+\frac{\partial u_j}{\partial a_k}+\frac{\partial u_l}{\partial a_j}\cdot\frac{\partial u_i}{\partial a_k}\right), \quad \cdots\cdots\cdots \quad (5)$$

Piezoelectric polarization is defined by

$$P_i=\alpha_{ijk}\cdot u_{jk}+\beta_{ijkl}\cdot\frac{\partial^2 u_i}{\partial a_j\cdot\partial a_k}, \quad \cdots\cdots\cdots \quad (6)$$

where β_{ijkl} are the fourth rank tensors that differ from zero in media that possess a center of symmetry. Thus piezoelectric polarization occurs in media that possess centers of symmetry. Wood can be approximated as a media with a center of symmetry, so that the second term of Equation (6) remains even if the strain is inhomogeneous. This piezoelectric polarization causes the observed peak in the *P-D* curve.

4. CONCLUSION

This paper investigated the piezoelectric phenomenon caused by deformation processes and the relationship between the piezoelectric voltage and microscopic fractures. In particular, the deformation of the cross-sectional wall of a tracheid under combined compression and vibration stresses was examined. By applying these stresses to a specimen, the cross-sectional walls of tracheids were deformed mainly at the radial walls. As soon as the radial wall buckled, the slope of the *P-D* curve changed, forming a convex curve. The maximum point on the *P-D* curve almost corresponded with the proportional limit of the *L-D* curve. In the non-elastic region, the piezoelectric voltage decreased slowly as the deformation progressed. During this time, the *L-D* curve became more curved. Finally, a clear peak appeared in the *P-D* curve, corresponding to a fracture along the boundary of the annual ring. This peak could be explained using the propagation theory of acoustic waves in inhomogeneous fields.

REFERENCES

1. Nakai, T. and Takemura, T., Mokuzai Gakkaishi, 39 (1993) 265-270.
2. Nakai, T., Igushi, N., and Ando, K., J. Wood Sci., 44 (1998) 28-34.
3. Nakai, T. and Ando, K., J. Wood Sci., 44 (1998) 255-259.
4. Nakai, T., Hamatake, M., and Nakao, T., J. Wood Sci., to be contributed.
5. Kogan, Sh. M., Soviet Physics-Solid state., 5(10) (1998) 2069-2070.
6. T. Ikeda, "Fundamentals of Piezoelectric Materials Science", 21-23 (1984) Ohm sha, Ltd., Tokyo.

(Received October 11, 2003; Accepted December 11, 2003)